

CO adsorption and thermal stability of Pd deposited on a thin FeO(1 1 1) film

R. Meyer, D. Lahav, T. Schalow, M. Laurin, B. Brandt,
S. Schauermaun, S. Guimond, T. Klüner, H. Kühlenbeck,
J. Libuda, Sh. Shaikhutdinov *, H.-J. Freund

Department of Chemical Physics, Fritz-Haber-Institut der Max-Planck-Gesellschaft, Faradayweg 4-6, Berlin 14195, Germany

Received 11 March 2005; accepted for publication 3 May 2005

Available online 31 May 2005

Abstract

We have studied adsorption of CO on Pd deposited on a thin FeO(1 1 1) film grown on a Pt(1 1 1) substrate using temperature programmed desorption, infrared reflection absorption spectroscopy and molecular beam techniques. At sub-monolayer Pd coverage, where formation of Pd(1 1 1) single layer islands upon heating is suggested on the basis of scanning tunneling microscopy studies, the CO desorption temperature is 70–100 K lower than on a Pd(1 1 1) single crystal, which agrees well with the results of ab initio calculations. However, annealing to 600 K results in strong reduction of the CO adsorption capacity, which is rationalized in terms of significant Pd migration through the film as revealed by angular resolved photoelectron spectroscopy measurements using synchrotron radiation. The results demonstrate the complexity of Pd interaction with the thin FeO(1 1 1) film at elevated temperatures.

© 2005 Elsevier B.V. All rights reserved.

Keywords: Palladium; Carbon monoxide; Oxide films; Iron oxides

1. Introduction

Metal particles deposited on thin oxide films have been shown to be suitable model systems

for studying structure–reactivity relationships of oxide supported metal catalysts [1–3]. In order to study reactivity of these systems at elevated temperatures, a detailed understanding of their thermal stability is a crucial prerequisite. Typically, annealing causes sintering of the particles and restructuring of their surfaces. Also, it can induce strong interactions with the support such as encapsulation and metal migration into the support

* Corresponding author. Tel.: +49 30 841 34114; fax: +49 30 841 34105.

E-mail address: shaikhutdinov@fhi-berlin.mpg.de (Sh. Shaikhutdinov).

[4–6], and references therein). The thermal stability, of course, depends on the nature of the oxide film and of the deposited metal.

Recently, on the basis of atomically resolved STM studies, we have reported that Pd particles deposited on an FeO(111) thin film on Pt(111) wet the oxide surface upon heating and form extended single layer islands [7,8]. Theoretical calculations have suggested that the wetting phenomena is induced by a strong interaction between Pd and the underlying support which arises in order to reduce the polar instability of the (111) surface of oxides with rocksalt crystal structure [8–10]. Inspired by this observation, we have suggested using this system for studying the effect of dimensionality on the adsorption properties of the metal deposits, i.e. two-dimensional islands vs. three-dimensional particles and single crystals.

In this paper, we studied the adsorption of CO on the Pd/FeO(111)/Pt(111) system using infrared reflection absorption spectroscopy (IRAS), temperature programmed desorption (TPD) and molecular beam (MB) techniques. Photoelectron spectroscopy (PES) with synchrotron radiation excitation was used for analysis of the surface composition in addition to scanning tunneling microscopy (STM) for structural analysis. Density functional theory (DFT) calculations were employed to aid in an understanding of the adsorption behavior observed.

2. Experimental

The studies were performed in three different UHV chambers: “STM + TPD” [7], “IRAS + MB” [11], and “PES” at BESSY II (Berlin). All chambers (base pressure below 3×10^{-10} mbar) were equipped with facilities for sample cleaning and heating, as well as with Auger electron spectroscopy/low energy electron diffraction optics (AES/LEED). Identical preparation conditions in each chamber were used to combine the results obtained in different chambers.

Fe and Pd were vapor deposited with commercial evaporators (Focus EFM3), which were calibrated with a quartz microbalance.

For the FeO film preparation, about one monolayer (ML) of Fe (99.99%, Goodfellow) was evaporated onto a clean Pt(111) substrate and subsequently oxidized in ca. 10^{-6} mbar O_2 at 1000 K for 2 min [12]. The absence of holes in the FeO film was checked by observation of characteristic LEED pattern and by the absence of CO adsorption signals in TPD or IR absorption spectra.

Palladium (99.99%, Goodfellow) was deposited on the oxide film at 90–100 K with a deposition rate of ca. 0.5 \AA min^{-1} . The Pd coverage was measured in nominal thickness (2.3 \AA corresponds to 1 ML). For each sample, a new film was grown.

TPD spectra were taken with a linear heating rate 5 K s^{-1} using a feedback control system.

IRAS spectra were taken with a Bruker IFS66v/S spectrometer with a resolution of 2 cm^{-1} . The spectra were referenced to spectra taken on the clean samples before CO dosage.

For the PES studies, we used the synchrotron facilities at BESSY II (beamline UE52-PGM1). The spectra were taken with a Scienta SES200 analyzer. In order to increase surface sensitivity, the Pd 3d, O 1s and Fe 2p regions were measured at photon energies such that the kinetic energy of the emitted electrons for each element was around 100 eV (with a total resolution around 0.1 eV). In addition, the photoelectrons were collected at two angles, 0° and 70° with respect to the surface normal. The energy was calibrated via the binding energy of the 4f levels of a clean Au foil.

MB experiments were performed in a molecular beam apparatus described previously [11], using a supersonic beam source and a non-line of sight quadrupole mass spectrometer (Extrel).

DFT calculations utilized a commercial version of the CASTEP program available as a module of Cerius² [13]. The FeO/Pt(111) film was simulated by a slab model containing 4 layers of Pt and one layer of Fe and O stacking as O–Fe–Pt(4) in (1×1) unit cell (three atoms per layer), using the PBE exchange-correlation functional [14] and ultrasoft non-local pseudopotentials [15]. A plane wave cutoff of $E_{\text{cut}} = 400 \text{ eV}$ turns out to be sufficiently accurate. The surface Brillouin zone was sampled by eight special k -points. The Pd atoms were set directly above oxygen of the FeO layer

as previously found [8]. CO adsorption was calculated for 0.33 ML coverage. To calculate CO adsorption on bulk Pd, a four layer slab of Pd(111) was used.

3. Results and discussion

3.1. Temperature programmed desorption

Fig. 1 shows the CO TPD spectra observed for Pd as deposited on the FeO(111) film at 90 K (a) and those measured in the second TPD experiment (b) over the same sample as a function of Pd coverage. (Note, that no further changes were detected in the consecutive spectra and the clean FeO films are stable in vacuum up to 900 K, at least.) The results clearly show that CO adsorption is strongly affected by the first heating, and the effect is greater for the smaller Pd coverage as shown in Fig. 1c. This implies that the morphology of the Pd deposits changes on heating to 600 K, which is consistent with our previously published STM results [7].

TPD and IRAS studies on CO adsorption on Pd crystal surfaces showed that weakly bound linear (or atop) CO species desorb first, resulting in a broad TPD signal at 100–300 K [16]. As the CO coverage decreases on heating, the remaining molecules occupy the more favorable bridge and three-fold hollow sites from which they desorb at a higher temperature with a well-resolved maximum at ~ 470 K for Pd(111).

The shape of the spectrum observed for the annealed Pd/FeO sample at 5 Å coverage (~ 2 ML) is indeed similar to that for a Pd(111) single crystal. However, at sub-monolayer coverage, the desorption maximum gradually shifts to temperatures as low as 360 K, with concomitant loss of intensity.

Such a behavior is very different from that observed for Pd deposited on the 5–10 nm thick Fe₃O₄(111) films, where annealing affects only the low temperature (100–300 K) part of the TPD spectra, keeping the high temperature part (400–500 K) practically unchanged [17]. The results for Pd/Fe₃O₄ can be explained by sintering of small and hence rough particles, formed at low deposition temperature, and/or smoothing of

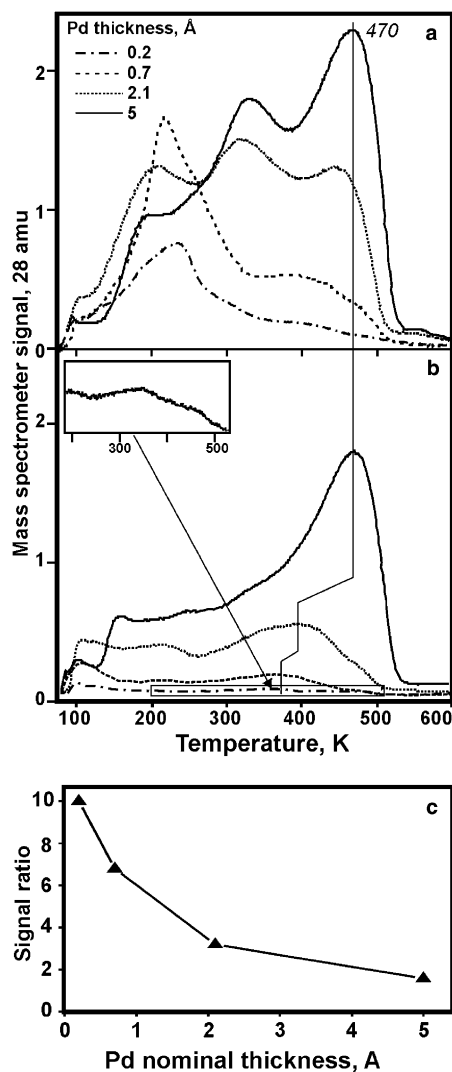


Fig. 1. First (a) and second (b) CO TPD spectra for Pd deposited on FeO(111)/Pt(111) at 90 K as a function of Pd coverage (in Å). For each spectrum, the exposure was 1 L of CO at 90 K. The ratios of integral CO TPD signals (first/second) are shown in (c).

the Pd surface on heating. Both effects favor CO adsorption in the most strongly binding hollow sites present on the particle facets.

In contrast to the Pd/Fe₃O₄(111) system, where the Pd deposits always exhibited a three-dimensional morphology, high resolution STM studies of the annealed Pd/FeO(111) surface showed formation of two-dimensional, single layer islands,

which were previously assigned to Pd(111) monolayer structures [7,8]. Therefore, a difference between two systems in CO adsorption could in principle be attributed to the different morphology of the Pd deposits on these iron oxide supports. This would imply that Pd(111) monolayer islands adsorb CO weaker than the Pd(111) crystal and Pd particles (T_{des} shifts to the lower temperatures), thus indicating an effect of dimensionality on the adsorption properties of Pd.

3.2. Infrared reflection–absorption spectroscopy and molecular beam study

In order to determine CO adsorption sites, we have employed IRAS. A large database exists on the stretching frequencies of differently coordinated CO (see e.g. [16,18–21] and references therein). For example, CO on the Pd(111) crystal surface preferentially adsorbs at threefold hollow sites resulting in the IRAS signals between 1820 and 1920 cm^{-1} with a continuous shift toward higher frequencies as the CO coverage increases.

Accordingly, a peak at $\sim 1960 \text{ cm}^{-1}$ is assigned to bridge-bonded CO, which emerges at intermediate coverage. Finally, at saturation coverage reached at low temperatures (around 100 K), atop species are populated giving rise to a signal at $\sim 2110 \text{ cm}^{-1}$.

Fig. 2a shows IRAS spectra of the sample exposed at 100 K to CO (1 Å of Pd deposited on the FeO film at 100 K in this case), which exhibits an intense peak at 2115 cm^{-1} and a relatively broad signal centered at 1960 cm^{-1} . The peak at 2115 cm^{-1} can be assigned to CO linearly adsorbed on Pd clusters. The abundance of atop species for “as deposited” sample is consistent with TPD results where CO mostly desorbs at 100–300 K associated with weakly bonded linear CO. The signal around 1960 cm^{-1} was in a similar case assigned to bridge bonded CO mainly adsorbed at defect sites such as particle edges [21].

After annealing to 600 K, both signals are strongly attenuated (by factor of ~ 4). This observation is in line with the TPD results showing that the CO adsorption capacity strongly decreases (see Fig. 1c). The atop peak from the as deposited sam-

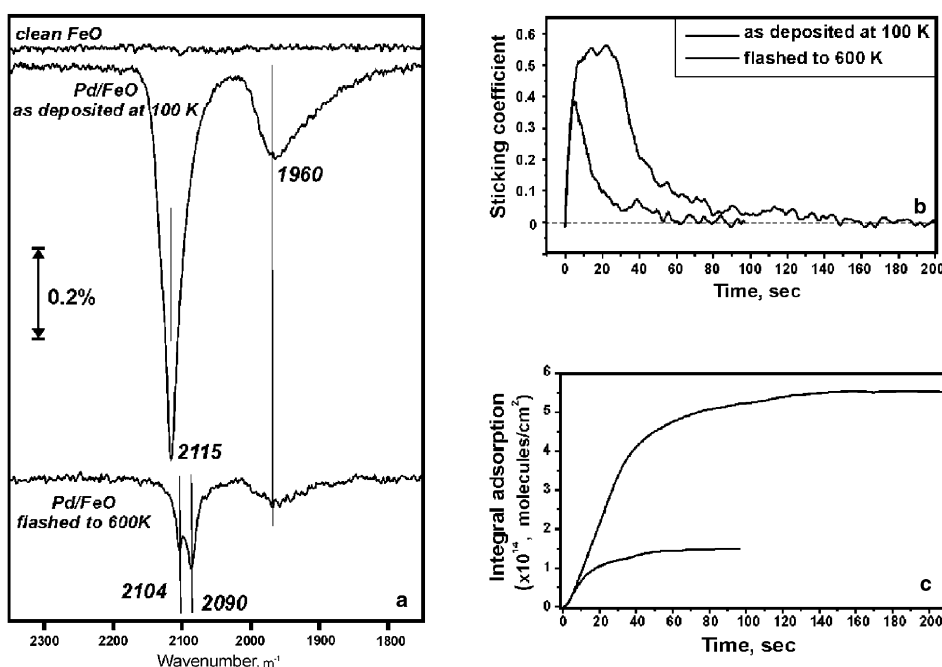


Fig. 2. (a) IRAS spectra of CO adsorbed at 100 K on 1 Å Pd deposited on FeO at 100 K and annealed to 600 K. Sticking coefficient (b) and integral CO adsorption (c) for the same samples as in (a) measured in molecular beam experiments.

ple is slightly red-shifted and can be deconvoluted into two features centered at 2104 cm^{-1} and 2090 cm^{-1} . The shift can be explained by the reduction of CO saturation coverage on Pd [20]. The 2090 cm^{-1} peak coincides with that observed for CO adsorbed on small Pt “holes” on the clean FeO film (if they were present), but it may also be due to atop CO species at special Pd sites.

These findings are corroborated by molecular beam experiments. On the as deposited Pd particles, the sticking coefficient shows a typical precursor-type behavior (see Fig. 2b). The sticking probability remains high and nearly constant until it drops rapidly when reaching the saturation coverage. Note that the absolute value of the sticking coefficient may be overestimated due to the so-called “capture zone” effect, i.e. trapping on the oxide support and subsequent surface diffusion of the adsorbate to the Pd particles ([22,23] and references therein). The amount of CO adsorbed can be quantified via integration of the sticking probability at a known beam flux as shown in Fig. 2c. Integration yields a CO density of 0.55×10^{15} molecules/cm², which at a nominal Pd coverage of 0.67×10^{15} molecules/cm² (equivalent to 1 Å Pd coverage) corresponds to a CO/Pd ratio around 0.8. This value is consistent with the maximum coverage of 0.75 observed on Pd(111) [19], taking into account that on very small particles the CO adsorption capacity may be enhanced due to the high density of low coordinated sites such as edges and corners.

After annealing to 600 K, the adsorption capacity drops to ~25% of its original value. Assuming that all Pd atoms form monolayer islands upon annealing, this gives the CO saturation coverage on Pd around 0.22. This finding is consistent with the IRAS results discussed above. Note that the relatively high initial sticking coefficient of ~0.4 (see Fig. 2b) does not imply a high density of adsorption sites, but may be consequence of the “capture zone” effect.

3.3. Density functional theory

In order to aid in an understanding of CO adsorption on monolayer islands, we have performed DFT calculations.

As a starting point, the CO adsorption energy on a four-layer Pd slab with a lattice constant of 2.76 Å was calculated as a confirmation that our method accurately predicted bulk behavior. The results show that CO prefers to adsorb in threefold hollow sites in agreement with experiments. An adsorption energy of 2.25 eV also agrees well with earlier calculations [24].

Then we considered a model consisting of a relaxed Pd–O–Fe–Pt(4) slab with interlayer distances equal to 2.3 Å for Pd–O and 0.65 Å for O–Fe, and the Pd atoms occupying the atop sites with respect to the O layer [8]. Note that, in order to reduce the numerical effort of the calculations, the lattice constant of the Pt(111) substrate was extended from 2.77 Å to 3.09 Å in order to match the FeO(111) layer, which is similar to the assumptions made in [25].

Within this approach, the calculations predict that CO adsorbing in the threefold hollow site is energetically favorable, and the binding energy of CO in this site is calculated to be 2.03 eV, a difference of 0.22 eV as compared to the slab of Pd(111). This result is in agreement with TPD data, which revealed lowering of the desorption temperature to ~400 K for 1 ML Pd coverage (see Fig. 1b).

We then examined CO adsorption on a free-standing monolayer of Pd (with the lattice constant 2.76 Å as in Pd(111)) to determine if the reduction in binding energy was merely related to an effect of reduced dimensionality. However, we found an increase in the binding strength to 3.35 eV. The lattice expansion (from 2.76 Å to 3.09 Å as in Pd/FeO(111)) is found to increase threefold hollow site CO adsorption energy by ~0.6 eV. Both results contradict the experimental data, thereby indicating that the support is indeed quite important for the bonding in this system.

Within this calculation we have examined whether a charge transfer occurs between Pd and oxide. Our calculations did not reflect a charge transfer such as that found for Pd/MgO(111) where a significant positive charge on Pd ($+0.26e^-$) was observed [10]. However, important differences between the two systems exist. Namely, we have layers of Pt(111) underneath FeO(111),

which provides a large reservoir by which the polarity of the FeO surface can be quenched. Meanwhile, a bulk MgO(111) crystal has been considered in [9,10] and therefore any charge quenching must come from the Pd monolayer. Indeed, when we have performed calculations for Pd on a FeO(111) crystal as opposed to a thin film, we also observed a positive charge on Pd of $+0.14e^-$. Therefore, based on our results for the thin film, the concept of a charge transfer cannot be used to explain the adsorption behavior of the Pd monolayer on FeO(111).

In summary, the DFT calculations predict that, for the system consisting of a Pd monolayer on top of FeO(111)/Pt(111), CO molecules should efficiently adsorb on hollow sites, but with a lower adsorption energy, which agrees well with the desorption temperature measured by TPD. The effect can be assigned to redistribution of electron density within Pd layer. However, the calculations

cannot explain the experimental observation of strong reduction of CO saturation coverage on the annealed Pd/FeO surface.

3.4. Photoelectron spectroscopy

The results presented above lead us to the situation where either the model of Pd(111) single layer islands has to be reconsidered or, in contrast to the theoretical predictions, the charge transfer really occurs, which could in principle explain weak CO adsorption (metal oxides are known to adsorb CO much weaker than metals). In order to study both the electronic structure and surface composition of Pd/FeO we employed photoelectron spectroscopy with synchrotron radiation.

Fig. 3 shows spectra observed for 1 Å coverage of Pd deposited at 90 K. The Pd 3d region recorded immediately after deposition shows a $3d_{5/2}$ peak centered at binding energy (BE)

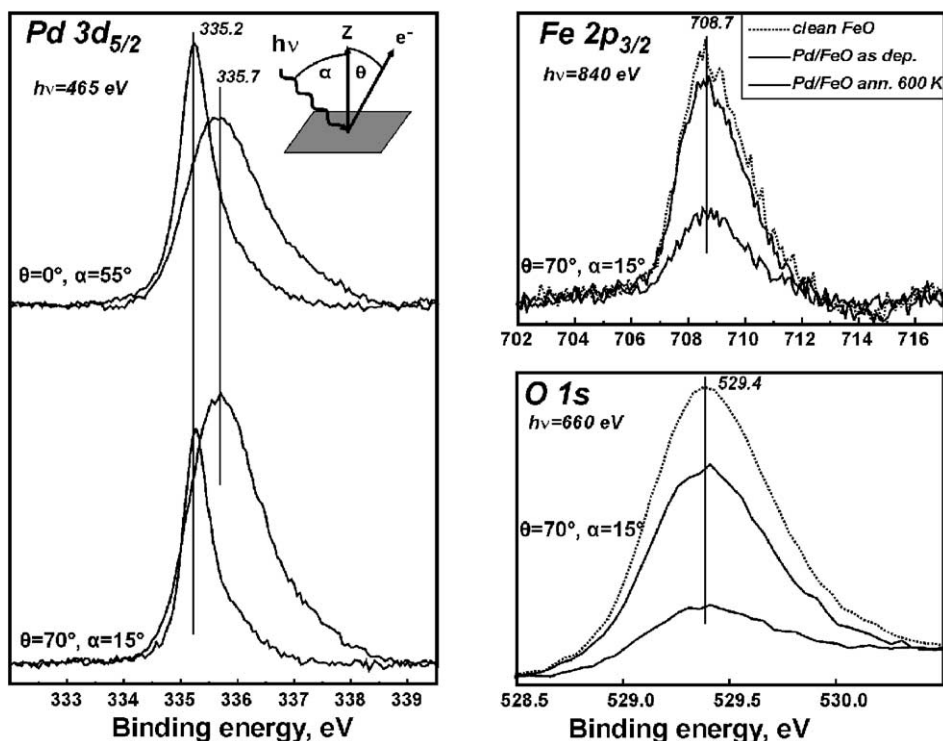


Fig. 3. Photoelectron spectra observed for 1 Å Pd deposited on FeO at ~ 90 K (black lines) and then annealed to 600 K (gray). The Fe and O signals for the clean FeO film (dotted lines) are shown for comparison. The spectra for Pd 3d region are measured at two angles (0° and 70°) with respect to the surface normal.

335.7 eV, i.e. about 0.5 eV higher than for Pd bulk systems. The BE shifts can be assigned to the particle size effects well documented for oxide supported metal particles [3]. The relatively broad peak (a half-width is ~ 1.6 eV) reflects the size distribution of the Pd particles.

After heating to 600 K, the signal became much narrower (a half-width is reduced to ~ 0.6 eV) and shifted to 335.2 eV, i.e. typical for the Pd bulk. When measured at normal angle, the integrated signal is decreased by 30% as compared to the as deposited sample. However, for the grazing angle measurements, the signal area is reduced by factor of ~ 2.5 . This means that the amount of Pd on the surface strongly decreases upon heating. Meanwhile, the Fe and O signals for the annealed sample increased by factor of 2.4 and 2.1, respectively, and almost recover to the intensities of the clean FeO surface before Pd deposition. These results can only be rationalized by assuming that Pd migrates through the FeO film. If the Pd particles only wet the oxide film, one would expect decrease rather than increase of the signal from the oxide support, in contrast to the experimental results. Also the observation of the BE value typical for the Pd bulk systems indicates that Pd may be in direct contact with the metal (Pt) substrate.

3.5. Scanning tunneling microscopy (revisited)

Pd migration through the film to the FeO/Pt(111) interface, revealed by PES, implies that the monolayer islands imaged by STM on the annealed surfaces may be FeO in nature, with encapsulated Pd islands underneath. Since the clean FeO film does not adsorb CO above 90 K, this surface would be expected to be inert towards CO, which could explain the strong reduction of CO adsorption capacity.

Therefore, we have performed additional STM studies on this system. Basically, the results are very similar to those we have previously reported [7]. However, two interesting features have been observed on the annealed surfaces, which are mentioned below.

First, we have found that, in addition to the monolayer islands, there are ill-defined structures with apparent height of ~ 1 Å with respect to the

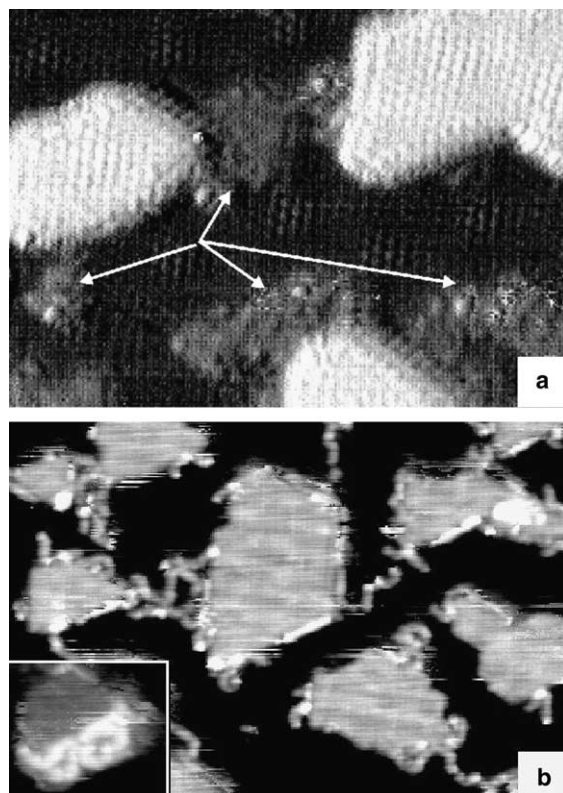


Fig. 4. STM images of ~ 1 Å Pd deposited at 130 K on the FeO(111) film and flashed to 600 K. Islands of 0.25 nm in height are atomically resolved. The arrows show ill-defined structures of ~ 0.1 nm in height. “Worm”-like structures, which are a single atom wide, are observed in (b). The inset shows their presence on top of islands as well. The images are presented with differentiated contrast. Size and image parameters: (a) 16×11.5 nm, $V_t = -20$ mV, $I = 2.9$ nA and (b) 37.5×25.5 nm, $V_t = -200$ mV, $I = 1.9$ nA.

FeO layer, as shown in Fig. 4a, which were not seen on the clean film and the Pd covered surface before annealing. In principle, these features could be the result of Pd migration into the film, followed by growth of Pd islands in the subsurface region. This interpretation would be in line with the PES results.

Second, we have observed a number of times single layer islands, which exhibit atomic “worm”-like structures, as shown in Fig. 4b. It appears that this image has captured the processes occurring upon heating. It seems unreasonable that Pd particles diffuse intact through the FeO

film. This suggests that any diffusion must occur on atom by atom basis. Therefore, STM observation of the large and well shaped single islands (see Fig. 4a) implies relatively fast diffusion of the Pd atoms on the Pt(111) substrate *underneath* the FeO layer. On the other hand, such a process would have to be accompanied by strong deformations of oxide surface and therefore characterized by large activation barriers, which may result in kinetically limited, metastable structures such as imaged in Fig. 4b. Interestingly, that similar features are observed on the top of islands as well (see the inset).

The STM images, presented in Fig. 4, show that different processes may occur simultaneously on heating to elevated temperatures.

4. Concluding remarks

The present study, employing various experimental techniques, shows that Pd particles deposited on an ultra-thin FeO(111) film grown on a Pt(111) substrate possess limited thermal stability. After deposition small Pd particles exist on the FeO(111) surface, which exhibit typical CO adsorption properties for small Pd particles. After annealing to 600 K, the Pd/FeO system shows unusual CO adsorption behavior, which is the consequence of a complex interplay between several simultaneous processes. Therefore, the resulting surface may critically depend on the final temperature, heating and cooling rates, annealing time, etc.

The mechanism of the Pd migration and its driving force are unclear. Although the surface energy of the FeO/Pd/Pt system is expected to be lower than of Pd/FeO/Pt, theoretical calculations are necessary in order to obtain an estimate of the energy differences and the corresponding activation barriers.

The metal migration could in principle be driven by the high mutual affinity of Pt and Pd, sharing the same crystal structure and having almost identical lattice constants, which makes possible their alloying without immiscibility gap [26]. On the other hand, Au also readily forms alloys with Pt [26], but grows three-dimensionally on the

FeO film above 0.2 Å coverage and does not form monolayer islands on heating [27].

The present study demonstrates the complexity of the processes involving strong Pd interaction with the thin FeO(111) films at elevated temperatures.

Acknowledgments

We thank M. Sterrer and T. Risse for technical support and fruitful discussions. We acknowledge support by the Athena project funded by the Engineering and Physical Sciences Research Council (EPSRC) of the U.K. and Johnson Matthey plc, and also the EU Training Network “Catalysis by Gold” (TMR Auricat).

References

- [1] D.R. Rainer, D.W. Goodman, *J. Mol. Cat. A* 131 (1998) 259.
- [2] C.T. Campbell, *Surf. Sci. Rep.* 27 (1997) 1.
- [3] M. Bäumer, H.-J. Freund, *Prog. Surf. Sci.* 61 (1999) 127.
- [4] O. Dulub, W. Hebenstreit, U. Diebold, *Phys. Rev. Lett.* 84 (2000) 3646.
- [5] M. Bowker, P. Stone, R. Bennett, N. Perkins, *Surf. Sci.* 339 (2002) 155.
- [6] M. Heemeier, S. Stempel, Sh.K. Shaikhutdinov, J. Libuda, M. Bäumer, R.J. Oldman, S.D. Jackson, H.-J. Freund, *Surf. Sci.* 523 (2003) 103.
- [7] R. Meyer, M. Bäumer, Sh.K. Shaikhutdinov, H.-J. Freund, *Surf. Sci.* 546 (2003) L813.
- [8] Sh.K. Shaikhutdinov, R. Meyer, D. Lahav, M. Bäumer, T. Klüner, H.-J. Freund, *Phys. Rev. Lett.* 91 (2003) 076102.
- [9] J. Goniakowski, C. Noguera, *Phys. Rev. B* 60 (1999) 16120.
- [10] J. Goniakowski, C. Noguera, *Phys. Rev. B* 66 (2002) 085417.
- [11] J. Libuda, I. Meusel, J. Hartmann, H.-J. Freund, *Rev. Sci. Instrum.* 71 (2000) 4395.
- [12] W. Weiss, W. Ranke, *Progr. Surf. Sci.* 70 (2002) 1.
- [13] Cerius² is provided by Accelrys. Inc.
- [14] J.P. Perdew, K. Burke, M. Ernzerhof, *Phys. Rev. Lett.* 77 (1994) 3865.
- [15] D. Vanderbilt, *Phys. Rev. B* 41 (1990) 7892.
- [16] X. Guo, J.T. Yates Jr., *J. Chem. Phys.* 90 (1989) 6761.
- [17] R. Meyer, S.K. Shaikhutdinov, H.-J. Freund, *Z. Phys. Chem.* 218 (2004) 905.
- [18] J. Szanyi, W.K. Kuhn, D.W. Goodman, *J. Vac. Sci. Technol. A* 11 (1993) 1969.

- [19] F.M. Hoffman, Surf. Sci. Rep. 3 (1983) 107.
- [20] P. Hollins, Surf. Sci. Rep. 16 (1997) 51.
- [21] V. Yudanov et al., J. Phys. Chem. 107 (2003) 255.
- [22] C. Henry, Surf. Sci. Rep. 31 (1998) 231.
- [23] J. Hoffmann, S. Schauermann, J. Hartmann, V.P. Zhdanov, B. Kasemo, J. Libuda, H.-J. Freund, Chem. Phys. Lett. 354 (2002) 403.
- [24] B. Hammer, L.B. Hansen, J.K. Nørskov, Phys. Rev. B 59 (1999) 7413.
- [25] H.C. Galloway, P. Sautet, M. Salmeron, Phys. Rev. B 54 (1996) R11145.
- [26] H. Okamoto et al., Binary Alloy Phase Diagrams, second ed., ASM International, 1992.
- [27] C. Lemire, R. Meyer, Sh.K. Shaikhutdinov, H.-J. Freund, Surf. Sci. 552 (2004) 27.